# Preprocessor for Impulse Radio

Xufang Wang and Tung-Sang Ng, *Fellow, IEEE*

***Abstract*—A preprocessor for ultra-wideband (UWB) communications using impulse radio is proposed. The received UWB signal is divided into subband signals, which can be individually processed and recombined before demodulation of the signal. Perfect reconstruction of the pulses via analog subband processing is achieved. The division of subbands is flexible and the number depends on the number of frequency bands that requires processing. Only the subbands that require processing need to be digitized. The application of the preprocessor to interference cancellation is also demonstrated.**

***Index Terms*—Interference cancellation, preprocessor, ultra-wideband (UWB) communication.**

## I. Introduction

ONE OF the enabling techniques for ultra-wideband (UWB) communications is impulse radio. The impulse radio employs short-duration pulses, resulting in a signal having an ultrawide (several gigahertz) bandwidth. This radio system has to coexist with many existing communication systems transmitting on the same frequency band, for example, IEEE 802.11a wireless local area networks (WLANs) operating around 5 GHz. It is therefore advantageous to use an interference canceller that can pass the UWB pulses to the correlator/detector and, at the same time, filter out the strong interference from existing systems. One of the requirements of this canceller is to have a wide instantaneous bandwidth which means the sampling-rate requirement is very significant. To relax the sampling-rate requirement, a channelized receiver structure can be used. Two types of channelized receivers, originally proposed for the radio detection and ranging (RADAR) system, have been proposed for UWB receivers [1]. One is the time-domain channelized receiver [2], in which the input-bandwidth requirement for each analog-to-digital converter (ADC) is still determined by the bandwidth of the incoming signal. The other is the frequency-domain channelized receiver [1]. Although the sampling rate is reduced, it has the disadvantage that it is quite difficult to reconstruct the signal waveform. In fact, perfect reconstruction has not been realized in analog subband processing before [3]. Nevertheless, reconstruction of the impulses is important in the correlation and detection of signals for impulse radio. A frequency-domain channelized direct-sequence spread-spectrum UWB receiver has been proposed in [4]. The receiver can be practically implemented by employing down conversion through mixers cascaded with low-pass filters (LPFs). The mixing process produces the sum and the difference frequency components. Because of the wide bandwidth of the UWB signal with respect to the mixing frequency, both sum and difference frequency components take part in the low-pass filtering, causing spectrum overlap and distortion.

In this paper, a new impulse-radio preprocessor with reduced requirement on the sampling rate is proposed. Perfect reconstruction of the pulses via analog subband processing is achieved. The received UWB signal is divided into subbands, the number of which depends on the number of frequency bands that requires processing. Each subband signal can be individually processed, and all processed signals are recombined before demodulation at a later stage. The problem of signal spectrum overlap and distortion in [4] is avoided by employing successive subtraction of previous subband signals in the generation of next subband signals. Only the subbands that require processing, e.g., interference cancellation, need to be digitized. It is apparent that sampling rate requirement is greatly reduced. Various techniques [5]–[7] have been proposed for interference cancellation in UWB communications. However, all these approaches are digital and assume that the UWB signal has already been properly digitized. Cancellation of strong interference in [4] requires filters with long filter taps, and optimization of the synthesis filters could be difficult. As will be demonstrated later, the application of the preprocessor to narrowband or wideband interference cancellation is effective and robust.

This paper is organized as follows. The proposed preprocessor is described in Section II. Section III shows an example of the preprocessor and its application to interference cancellation. Finally, Section IV concludes the paper.

## II. Proposed Preprocessor

Referring to Fig. 1(a), the spectrum of the received UWB signal is divided into $M$ subbands and the preprocessor consists of $M$ branches each of which extracts a subband signal. Let $f_1$, $f_2, \ldots, f_{M-1}$ be the frequency division points for the subbands. That is, the spectrum is divided into $M$ subband signals having bandwidth of $f_1 - f_L, f_2 - f_1, \ldots, f_{M-1} - f_{M-2}, f_H - f_{M-1}$, where $f_L$ and $f_H$ are the lowest and highest frequencies of the UWB signal spectrum, respectively. There is no restriction on the bandwidth of individual subband. The division can be adapted to different situations. Let $f'_1, f'_2, \ldots, f'_{M-2}$ be the mixing frequencies for use in the extraction of the second, third, $\ldots, M-1$th subband signals. The $M$th subband is the residual frequency band that does not require processing. Note that in general, $f'_k < f_k$, $k = 1, \ldots, M-2$. As will be elaborated later, the difference between $f'_k$ and $f_k$ is the prereserved band to enable the use of filters without sharp cutoff characteristics, which can be practically implemented.

Manuscript received November 25, 2003; revised July 9, 2004; accepted July 26, 2004. The editor coordinating the review of this paper and approving it for publication is R. Murch.

The authors are with the Department of Electrical and Electronic Engineering, University of Hong Kong, Hong Kong (e-mail: xfwang@eee.hku.hk; tsng@eee.hku.hk).

Digital Object Identifier 10.1109/TWC.2005.852126

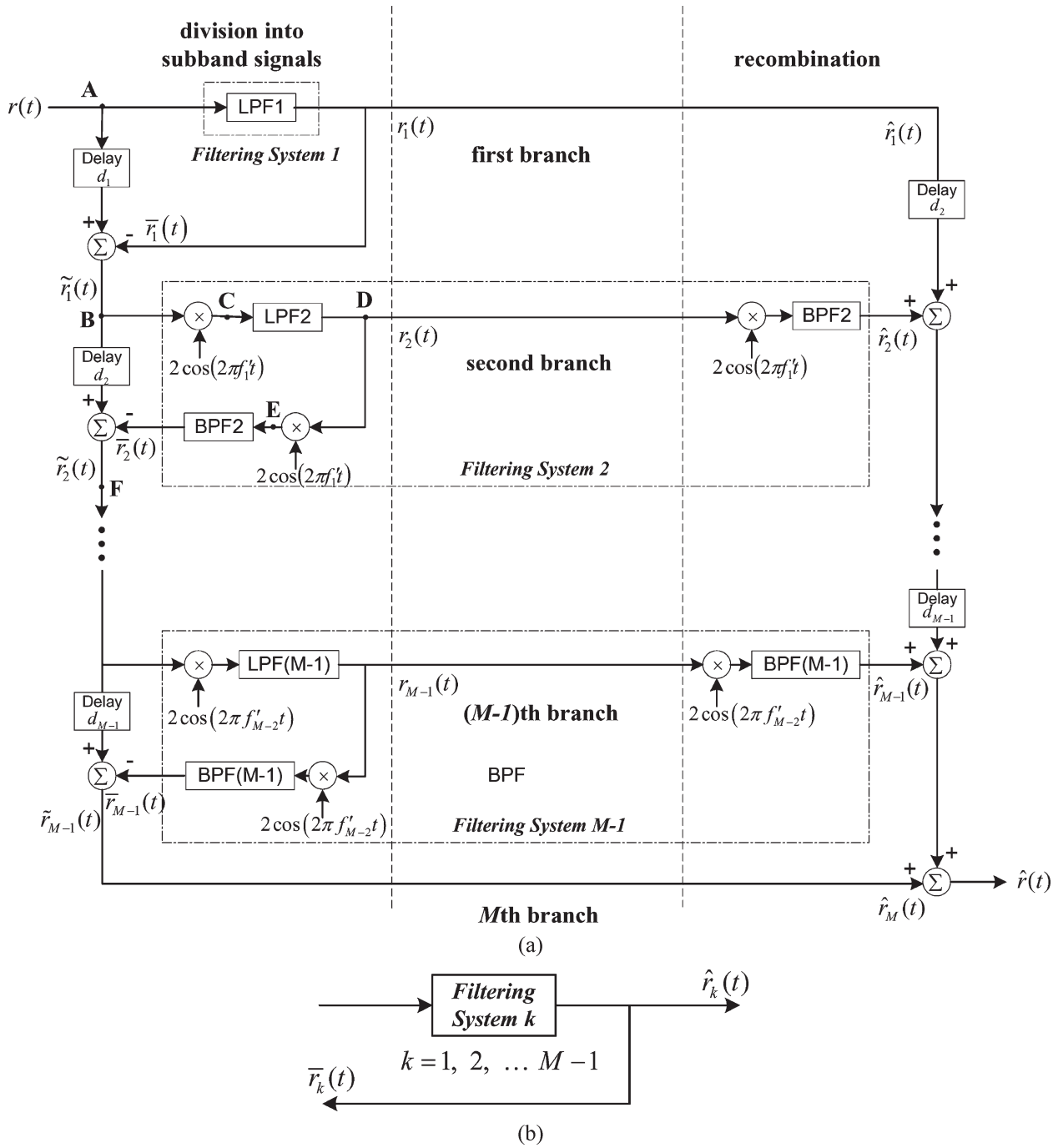


Fig. 1. (a) Proposed preprocessor. (b) Equivalent system of the filtering system $k$ in (a), $k = 1, 2, \ldots M-1$.

*First branch:*

The UWB signal $r(t)$ is first filtered by LPF1 with a passband $[0, f_1]$. The resultant first subband signal is $r_1(t)$. The signal $r(t)$ is delayed by $d_1$ seconds and then subtracted by $\overline{r}_1(t)$, where $\overline{r}_1(t) = \hat{r}_1(t)$, to yield $\tilde{r}_1(t)$. This subtraction is intended to remove the frequency components in $r(t)$ that are within the frequency range $[0, f_1]$. The delay $d_1$ is used to compensate for the delay introduced by LPF1 so that the subtraction between $r(t)$ and $\overline{r}_1(t)$ is coherent.

*Second branch:*

The signal $\tilde{r}_1(t)$ is frequency shifted by multiplying with $2\cos(2\pi f_1' t)$, wherein $f_1' < f_1$, so that the part of the spectrum $[f_1, f_2]$ of $\tilde{r}_1(t)$ is shifted down to the baseband $[f_1 - f_1', f_2 - f_1']$. The resultant signal is then filtered by LPF2 with a passband $[0, f_2 - f_1']$ to obtain the second subband signal $r_2(t)$. This signal $r_2(t)$ is multiplied by $2\cos(2\pi f_1' t)$ in order that the spectrum $[f_1 - f_1', f_2 - f_1']$ is shifted back to $[f_1, f_2]$. The resultant signal is then filtered by bandpass filter (BPF) 2 with a passband $[f_1, f_2]$, yielding $\overline{r}_2(t)$. This signal $\overline{r}_2(t)$ is fed back to the main path. On the main path, $\tilde{r}_1(t)$ is delayed by $d_2$ and the delayed signal is subtracted by $\overline{r}_2(t)$ to obtain $\tilde{r}_2(t)$. This subtraction is aimed at removing the frequency components of $\tilde{r}_1(t)$ on the band $[f_1, f_2]$. The delay $d_2$ is used

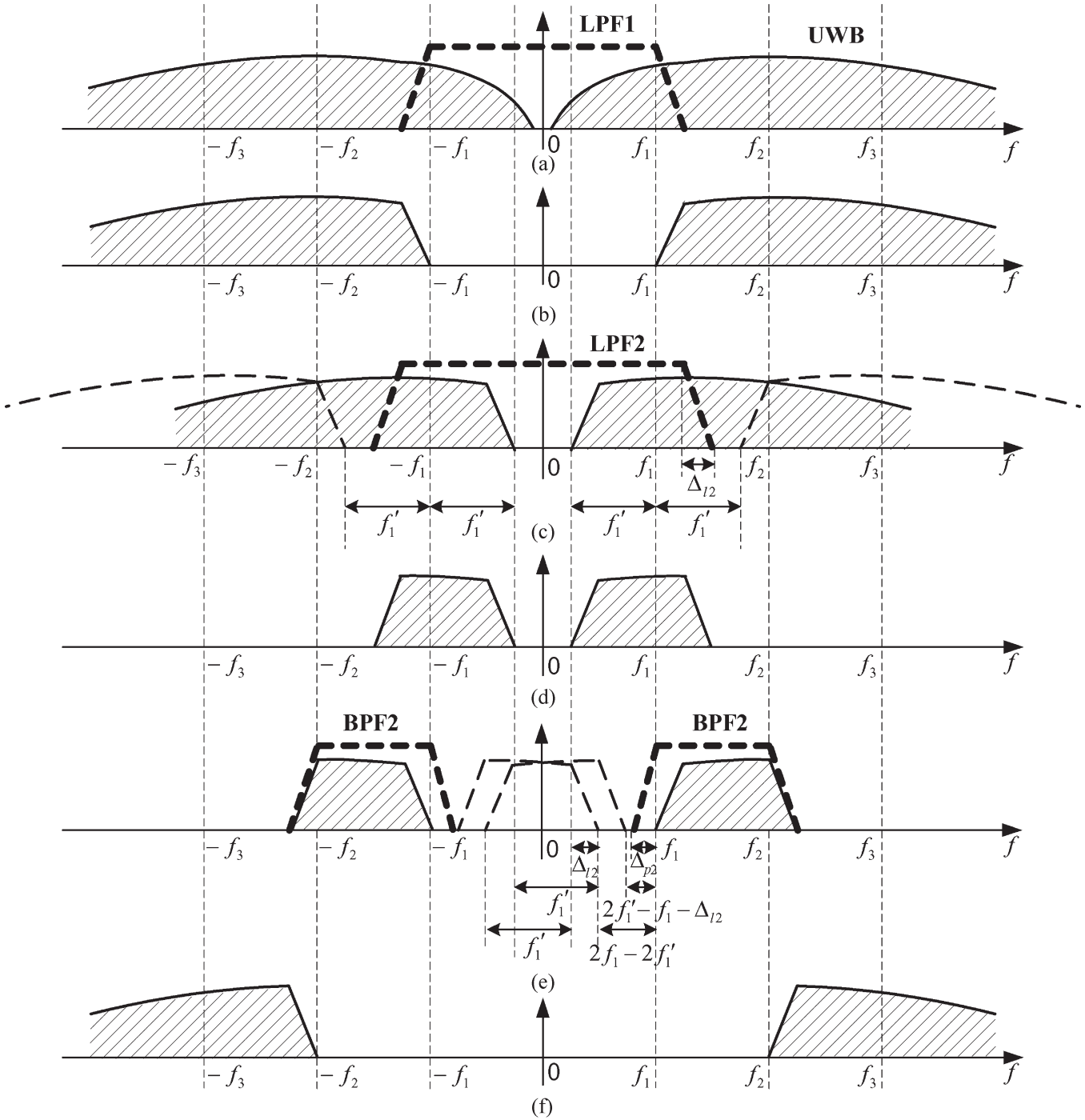


Fig. 2. Signal spectra at the points A–D and F of Fig. 1(a) are shown in (a)–(f), respectively. (a) Received UWB signal spectrum and LPF1. (b) Remaining signal spectrum after LPF1 is applied. (c) Signal spectrum in (b) is frequency shifted by $f_1'(f_1' < f_1)$ and LPF2. (d) Signal spectrum filtered out by LPF2. (e) Signal spectrum in (d) is frequency shifted by $f_1'$ and BPF2. (f) Difference between the signal spectrum in (b) and that filtered out by BPF2 in (e).

to compensate for the delay introduced by the cascade of LPF2 and BPF2.

*Other branches:*

The procedure is repeated until the $(M-1)$th branch is processed and the signal $\tilde{r}_{M-1}(t)$ is obtained, which is also the $M$th subband signal $\hat{r}_M(t)$.

The recombination of subband signals is as follows. The first subband signal is denoted as $\hat{r}_1(t)$. For $k = 2, 3, \ldots, M-1$, the $k$th subband signal $r_k(t)$ is multiplied by $2\cos(2\pi f_{k-1}' t)$ in order that the spectrum $[f_{k-1} - f_{k-1}', f_k - f_{k-1}']$ is shifted back to $[f_{k-1}, f_k]$. The resultant signal is then filtered by BPF$k$ with a passband $[f_{k-1}, f_k]$, yielding $\hat{r}_k(t)$. The signal $\hat{r}_1(t)$ is first delayed by $d_2$ seconds and is added to $\hat{r}_2(t)$. The resultant signal is delayed by $d_3$ seconds and then added to $\hat{r}_3(t)$. This process continues until $\hat{r}_{M-1}(t)$ is added. Afterwards, the resultant signal is added with $\hat{r}_M(t)$ to give the final output signal $\hat{r}(t)$.

### A. Proof of Perfect Reconstruction Property

By perfect reconstruction property means that the output signal $\hat{r}(t)$ is a delayed version of the input $r(t)$. Since $\overline{r}_k(t) = \hat{r}_k(t)$, $k = 1, \ldots, M-1$, the filtering systems in Fig. 1(a) is equivalent to the systems shown in Fig. 1(b). On the left side of Fig. 1(a), the following equations are noted:

$$\begin{aligned}
\tilde{r}_1(t) &= r(t-d_1) - \hat{r}_1(t) \\
\tilde{r}_2(t) &= \tilde{r}_1(t-d_2) - \hat{r}_2(t) \\
&= r(t-d_1-d_2) - \hat{r}_1(t-d_2) - \hat{r}_2(t) \\
&\vdots \\
\tilde{r}_{M-1}(t) &= r\left(t - \sum_{i=1}^{M-1} d_i\right) - \sum_{i=1}^{M-1} \hat{r}_i \left(t - \sum_{j=i+1}^{M-1} d_j\right) \qquad (1)
\end{aligned}$$

and on the right side

$$\hat{r}(t) = \tilde{r}_{M-1}(t) + \sum_{i=1}^{M-1} \hat{r}_i \left(t - \sum_{j=i+1}^{M-1} d_j\right). \qquad (2)$$

Note that the delay of the signal $\hat{r}_{M-1}(t)$ is $\sum_{j=M}^{M-1} d_j = 0$. Substituting (1) into (2), the following equation is derived

$$\hat{r}(t) = r\left(t - \sum_{i=1}^{M-1} d_i\right). \qquad (3)$$

It is apparent that $\hat{r}(t)$ is a delayed version of $r(t)$ with a delay $\sum_{i=1}^{M-1} d_k$, and this completes the proof.

The delays $d_k$, $k = 1, 2, \ldots, M-1$, are set as follows. If $k = 1$, for in-phase subtraction of $r_1(t)$, the signal $r(t)$ must experience a delay $d_1$ equal to the group delay of the LPF1; for $k = 2, 3, \ldots, M-1$, the need for in-phase subtraction of $r_k(t)$ requires that the signal $\tilde{r}_{k-1}(t)$ must experience a delay $d_k$ equal to the group delay of the LPF$k$ plus the group delay of the BPF$k$. The filters are required to have linear phases for in-phase subtraction of the signal. Surface acoustic wave (SAW) filters can be employed as they inherently exhibit linear phase and their amplitude and phase response can be independently controlled [8]. It follows that

$$d_k = \begin{cases} -\dfrac{d\angle H_{\mathrm{LPF}k}(j\omega)}{d\omega}, & k = 1 \\ -\dfrac{d\angle H_{\mathrm{LPF}k}(j\omega)}{d\omega} - \dfrac{d\angle H_{\mathrm{BPF}k}(j\omega)}{d\omega}, & k = 2, 3, \ldots, M-1. \end{cases} \qquad (4)$$

### B. Sensitivity Analysis of Imperfect Delays

Assume that the delay $d_2$ in the recombination part of the preprocessor is imperfect, and there is a deviation $\Delta d$ to the actual delay. Then the output signal $\hat{r}(t) = r(t - \sum_{i=1}^{M-1} d_i) + \Delta\hat{r}$, where the corresponding error $\Delta\hat{r} = \hat{r}_1(\tilde{t} + \Delta d) - \hat{r}_1(\tilde{t})$, $\tilde{t} = t - d_2 - d_3 - \cdots - d_{M-1}$. According to the Mean-Value Theorem, $\Delta\hat{r} = \hat{r}_1'(\xi)\Delta d$, where $\xi \in [\tilde{t}, \tilde{t} + \Delta d]$. For Gaussian monopulse $r(t)$ usually used to model the UWB pulse, the amplitude of $r(t)$ and $r'(t)$ is of the same order. The amplitude of $\hat{r}_1'(t)$ is smaller than that of $r'(t)$, since $\hat{r}_1(t)$ is the low-pass-filtered signal of $r(t)$, and it varies more smoothly than $r(t)$. The delay deviation $\Delta d$ is in the order of nanoseconds $(10^{-9})$, hence, the amplitude of $\Delta\hat{r}$ is at least nine order $(10^{-9})$ less than that of $r(t)$. The impact of $\Delta\hat{r}$ to the output signal $\hat{r}(t)$ can therefore be ignored and the same argument can be extended to other mismatch in delays. The insensitivity of the preprocessor to mismatch in delays has also been confirmed by extensive simulations.

TABLE I
PARAMETERS USED IN THE EXAMPLE OF THE PREPROCESSOR

| | $f_k$ (gigahertz) | $f_k'$ (gigahertz) | LPF$k$ Passband (gigahertz) | BPF$k$ Passband (gigahertz) | $d_k$ (nanosecond) |
|---|---|---|---|---|---|
| $k=1$ | 1.0 | 0.9 | 0–1 | — | 0.8300 |
| $k=2$ | 2.0 | 1.9 | 0–1.1 | 1–2 | 2.0140 |
| $k=3$ | 3.0 | 2.9 | 0–1.1 | 2–3 | 2.0440 |
| $k=4$ | 4.0 | 3.9 | 0–1.1 | 3–4 | 2.0540 |
| $k=5$ | 5.0 | 4.9 | 0–1.1 | 4–5 | 2.0540 |
| $k=6$ | 6.0 | — | 0–1.1 | 5–6 | 2.1027 |

Note that the perfect reconstruction property does not impose restrictions on the filters used, though the filters are preferred to have sharp cutoff characteristics to meet certain specifications in order to isolate the subband signals and avoid residual signal components from interfering with the generation of next subband signals. In the case of interference cancellation, the division can be implemented in a way that the interferences are placed in the passbands or stopbands of the filters but not their transition bands. The signal spectra at the points A–D and F of Fig. 1(a) are shown in Fig. 2(a)–(f), respectively. Let $\Delta_{lk}$ and $\Delta_{pk}$ denote the sizes of the transition bands of LPF$k$ and BPF$k$, $k = 2, \ldots, M-1$, respectively. To avoid the generation of the residual signal components due to signals falling on the transition band of BPF2, $\Delta_{p2}$ should be less than the smallest distance between the spectrum components as indicated in Fig. 2(e), i.e.,

$$0 < \Delta_{p2} < \min\left\{2f_1' - f_1 - \Delta_{l2}, 2f_1 - 2f_1'\right\}.$$

Thus, $\Delta_{l2}$ and the mixing frequency $f_1'$ are required to satisfy

$$\begin{aligned} 2f_1' - f_1 - \Delta_{l2} &> 0 \\ 2f_1 - 2f_1' &> 0. \end{aligned}$$

It yields the conditions

$$\begin{aligned} \frac{f_1 + \Delta_{l2}}{2} < f_1' &< f_1 \\ \Delta_{l2} &< 2f_1' - f_1. \end{aligned}$$

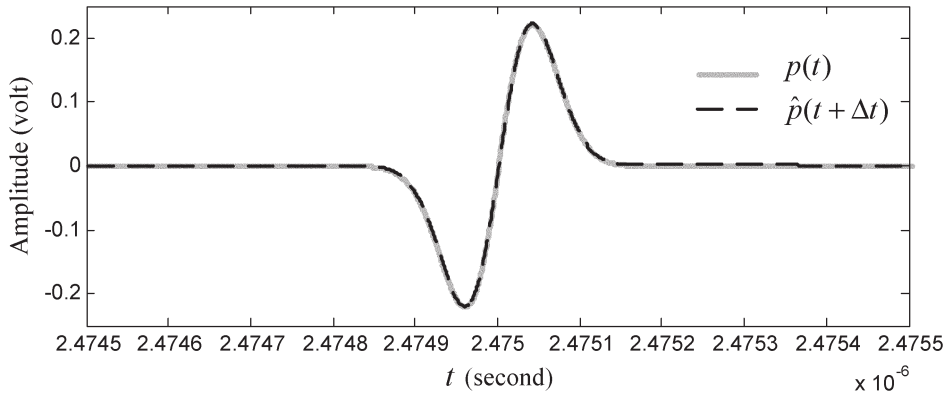


Fig. 3. Perfect reconstruction of the preprocessor, $p(t)$ is the received UWB pulse, $\hat{p}(t+\Delta t)$ is the corresponding pulse out of the preprocessor and $\Delta t = \sum_{k=1}^{6} d_k = 11.0987$ ns.

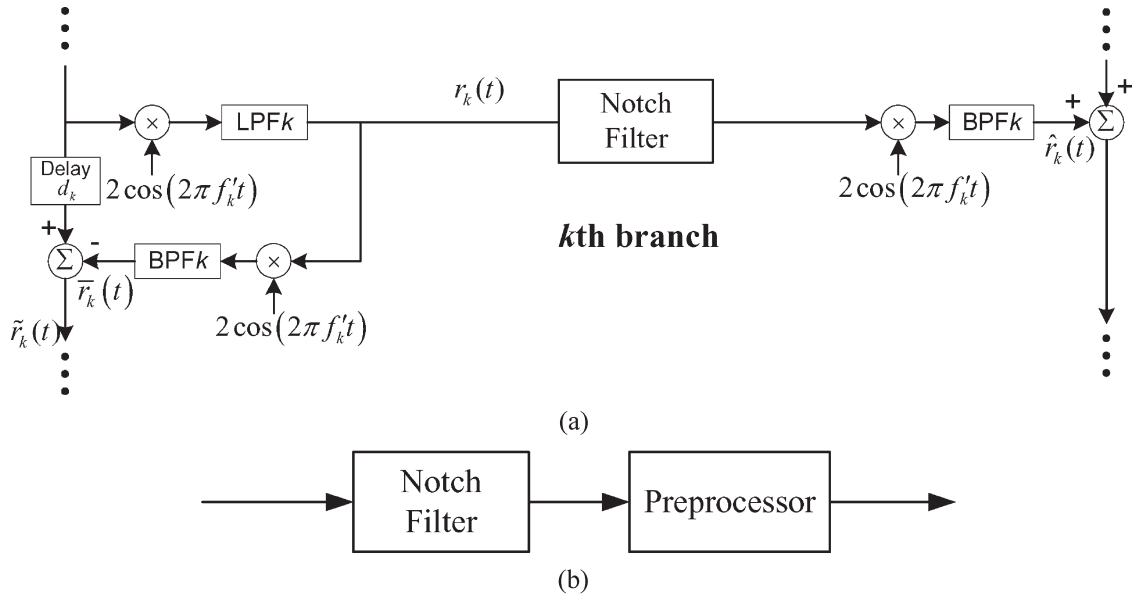


Fig. 4. (a) Notch filter is added to the $k$th branch of the preprocessor, $k = 1, 2, \cdots, M-1$. (b) Functionally equivalent system in (a).

These results can be extended to the rest of the $M-2$ branches. Thus, for $k = 2, \ldots, M-1$, $\Delta_{lk}$ and $\Delta_{pk}$ need to satisfy

$$\frac{f_{k-1} + \Delta_{lk}}{2} < f'_{k-1} < f_{k-1} \tag{5}$$

$$\Delta_{lk} < 2f'_{k-1} - f_{k-1} \tag{6}$$

and

$$\Delta_{pk} < \min\left\{2f'_{k-1} - f_{k-1} - \Delta_{lk}, 2f_{k-1} - 2f'_{k-1}\right\}. \tag{7}$$

## III. Example of the Preprocessor and Its Application

In the example, conventional analog filters are used instead of SAW filters for the purpose of demonstration. The number of branches of the preprocessor is $M = 7$. For $k = 1, 2, \ldots, M-1$ and $m = 1, 2, \ldots, M-2$, the frequency division points $f_k$, the delays $d_k$, the mixing frequencies $f'_m$, and the passbands of the LPFs and BPFs used are listed in Table I. The LPFs and BPFs are 11-order Chebyshev II filter with stopband attenuation 60 dB. Thus conditions (5)–(7) are satisfied. According to (1), each delay is set to the group delay or sum of the group delays at the center frequencies of the passbands of the corresponding filters (e.g., at 0.5 GHz of LPFs, 1.5 GHz of BPF1, etc.) as the phases of Chebyshev II filters are not quite linear. The sampling rate requirement is greatly reduced from over 14 GHz for received UWB signal (bandwidth prescribed by the Federal Communications Commission (FCC) [9] is 3.1–10.6 GHz) to

TABLE II
Parameters Used in the Example of Interference Cancellation

| | $f_k$ (gigahertz) | $f'_k$ (gigahertz) | LPF$k$ Passband (gigahertz) | BPF$k$ Passband (gigahertz) | $d_k$ (nanosecond) |
|---|---|---|---|---|---|
| $k=1$ | 5.0 | 4.9 | 0–5 | — | 0.1660 |
| $k=2$ | 6.0 | — | 0–1.1 | 5–6 | 2.1027 |

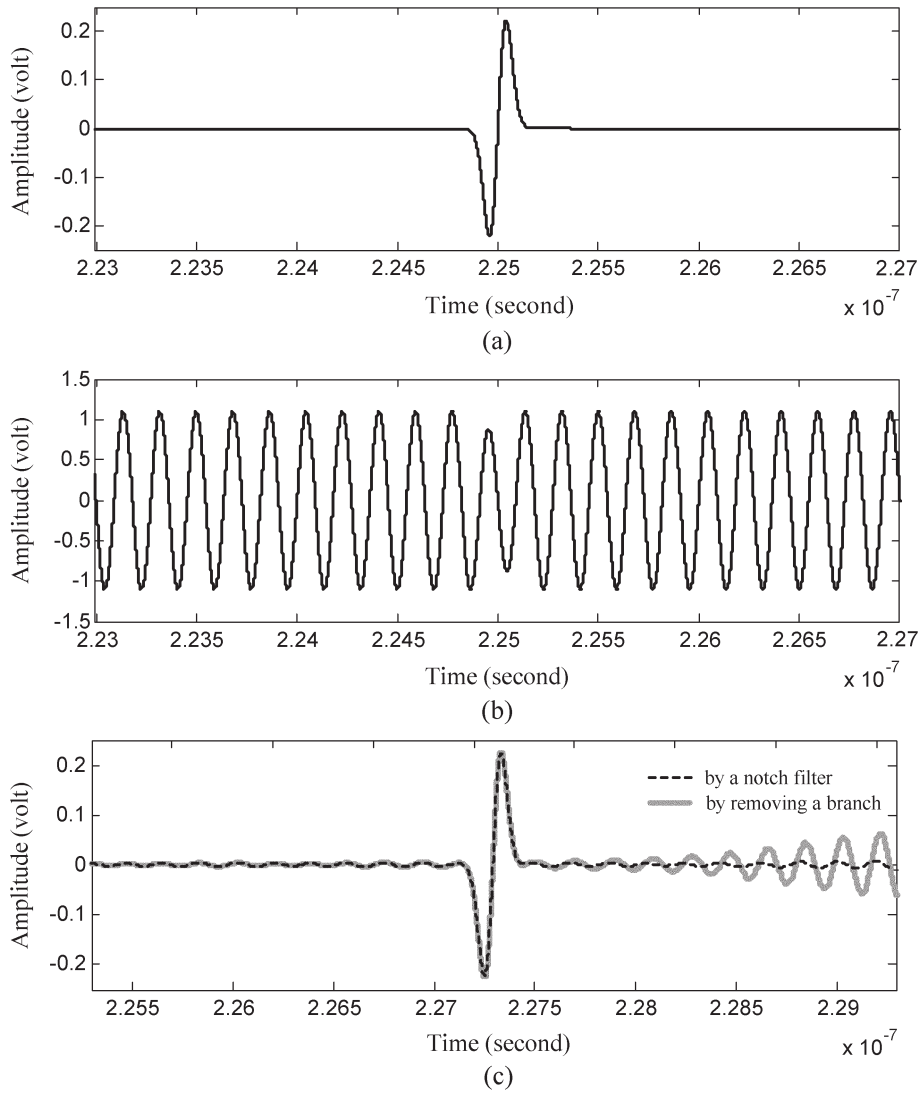


Fig. 5. Example of interference cancellation with the preprocessor. (a) UWB pulse without interference. (b) UWB pulse corrupted by BPSK interference. (c) UWB pulse out of the preprocessor after interference is removed.

about 2 GHz for each subband signal. By dividing into smaller subbands, the sampling rate requirement can be reduced even further.

One of the received UWB pulses simulated by Matlab, denoted by $p(t)$, is shown in Fig. 3. $p(t)$ is a Gaussian monopulse with a center frequency of 6.85 GHz. The corresponding pulse out of the preprocessor, denoted by $\hat{p}(t+\Delta t)$, is also shown in Fig. 3, which turns out to be the delayed version (delay $\Delta t = \sum_{k=1}^{6} d_k = 11.0987$ ns) of $p(t)$ as expected. The cross-correlation coefficient (normalized to unity) between the two pulses is $\rho_s = 1.0$.

The proposed preprocessor can be applied to signal processing, for instance, interference cancellation in impulse radio. The subband signals $r_k(t)$, $k = 1, 2, \cdots, M-1$, can be processed by notch or BPFs to remove interferences. Clearly, not all subband signals contain interferences. Only the subbands that require processing need digitization. So sampling rate requirement is greatly reduced. Fig. 4(a) shows the case when a notch filter is added to the $k$th branch of the preprocessor, which can be functionally equivalent to the system depicted in Fig. 4(b). This is because the notch filter is assumed not located in the transition bands. In the shifting operation, the notch position changes accordingly, and it does not affect the operation of the preprocessor. The notch filter can thus be moved outside the preprocessor. The effect of notch filtering on the UWB signal waveform can be predetermined and later incorporated into the template waveform of the correlator during demodulation. Referring to the previous example, suppose that the UWB pulses (pulse repetition rate $2 \times 10^7$ pulses/s) are corrupted by a narrowband interference modeled as a binary phase-shift keying (BPSK) signal, which is expressed as

$$i(t) = As(t)\cos(2\pi f_i t + \varphi)$$

where the interference amplitude $A = 1.1$, carrier frequency $f_i = 5.5$ GHz, and carrier phase $\varphi = 0$. The interference data bit $s(t) \in \{+1, -1\}$ with equal probability and bit rate is $1 \times 10^7$ bits/s. To show the design flexibility, the preprocessor above is changed to have only three branches ($M = 3$) with the parameters given in Table II. A second-order infinite-impulse

response (IIR) notch filter with the transfer function given by [10]

$$H(z^{-1}) = \frac{1 + \beta a z^{-1} + \beta^2 z^{-2}}{1 + \alpha a z^{-1} + \alpha^2 z^{-2}} \tag{8}$$

is then added to the second branch of the preprocessor, where $\alpha$ and $\beta$ are the coefficients controlling the pole and zero positions, respectively, and $a$ is the parameter controlling the position of the notch within the frequency spectrum. In the simulation, $\beta = 1.0$, $\alpha = 0.98$, and the center of the notch is placed at $f_i - f_5' = 5.5 - 4.9 = 0.6$ GHz. The delays are left unchanged due to the very small average group delay of this notch filter.

The UWB pulse without interference and interference-corrupted UWB signal are shown in Fig. 5(a) and (b), respectively. As the amplitude of the interference is much larger than the UWB pulse, the UWB pulse is overwhelmed and only little change in the BPSK signal waveform can be noticed. The signal-to-noise-and-interference ratio (SNIR) is $-38.3$ dB (noise ignored). The interference-corrupted UWB pulse bears little resemblance (the cross correlation coefficient $\rho_{si} = 0.012$) to the template pulse $p(t)$. After interference cancellation, the UWB pulse becomes clear as the interference is greatly suppressed, as shown in Fig. 5(c), with the cross correlation coefficient $\rho_{c1} = 0.98$ (notch effect is incorporated to the template) and SNIR increased to 17.5 dB.

The proposed preprocessor can also be applied to wideband interference. Instead of using notch filters, the branch that contains the wideband interference is discarded. For example, for the interference from WLAN signal covering 5.15–5.825 GHz, the whole second branch $\hat{r}_2(t)$ is discarded. It is clearly shown in Fig. 5(c) that the interference is also suppressed. Although there are higher ripples around the resultant pulse compared to the previous case (via a notch filter) due to loss of more signal spectrum, the effect of a branch loss can be incorporated into the template signal waveform of the correlator. Thus cross correlation coefficient between the resultant pulse and template is $\rho_{c2} = 0.99$.

Note that adding a notch filter or throwing away a branch can also be viewed as introducing imperfection and mismatch to the preprocessor. Therefore, the simulation results have demonstrated that the preprocessor is robust to imperfection and mismatch as well.

## IV. Conclusion

A preprocessor for UWB receivers has been proposed. The preprocessor divides the received UWB signal into subbands, and it has been proven that the recombined signal has perfect reconstruction property. As a consequence, the sampling rate requirement for digitally processing UWB signals is greatly reduced and its application to interference cancellation has also been demonstrated.

## References


[1] J. D. Taylor, *Ultra-Wideband Radar Technology*. Boca Raton, FL: CRC Press, 2001.

[2] G. T. Ruck, "Ultra-wideband radar receiver," in *Proc. SPIE*, Los Angeles, CA, 1992, vol. 1631, pp. 174–180.

[3] P. Lowenborg, H. Johansson, and L. Wanhammar, "Two-channel digital and hybrid analog/digital multirate filter banks with very low-complexity analysis or synthesis filters," *IEEE Trans. Circuits Syst. II, Exp. Briefs*, vol. 50, no. 7, pp. 355–367, Jul. 2003.

[4] W. Namgoong, "A channelized digital ultrawideband receiver," *IEEE Trans. Wireless Commun.*, vol. 2, no. 3, pp. 502–510, May 2003.

[5] E. Baccarelli, M. Biagi, and L. Taglione, "A novel approach to in-band interference mitigation in ultra wideband radio systems," in *Proc. IEEE Conf. Ultra-Wideband Systems and Technologies*, Baltimore, MD, 2002, pp. 297–301.

[6] D. Gerakoulis and P. Salmi, "An interference suppressing OFDM system for ultra wide bandwidth radio channels," in *Proc. IEEE Conf. Ultra-Wideband Systems and Technologies*, Baltimore, MD, 2002, pp. 259–264.

[7] I. Bergel, E. Fishler, and H. Messer, "Narrow-band interference suppression in time-hopping impulse-radio systems," in *Proc. IEEE Conf. Ultra-Wideband Systems and Technologies*, Baltimore, MD, 2002, pp. 303–307.

[8] C. K. Campbell, *Surface Acoustic Wave Devices for Mobile and Wireless Communications*. New York: Academic, 1998.

[9] *Revision of Part 15 the Commission's Rules Regarding Ultra-Wideband Transmission Systems,* Federal Commun. Commission (FCC), Washington, DC, ET Docket 98-153, 2002.

[10] J. F. Chicharo and T. S. Ng, "Tunable/adaptive second-order IIR notch filter," *Int. J. Electron.*, vol. 68, no. 5, pp. 779–792, 1990.